Dominant role of greenhouse-gas forcing in the recovery of Sahel rainfall

Article

Accepted Version

Dong, B. ORCID: https://orcid.org/0000-0003-0809-7911 and Sutton, R. ORCID: https://orcid.org/0000-0001-8345-8583
(2015) Dominant role of greenhouse-gas forcing in the recovery of Sahel rainfall. Nature Climate Change, 5 (8). pp. 757-760. ISSN 1758-678X doi: 10.1038/nclimate2664
Available at https://centaur.reading.ac.uk/40372/

Dominant role of greenhouse gas forcing in the recovery of Sahel rainfall

Buwen Dong and Rowan Sutton

National Centre for Atmospheric Science, Department of Meteorology, University of Reading

Six numerical experiments have been performed in this study using HadGEM3-A and they are summarized in Table S1. All experiments were integrated from the same initial conditions, taken from a 5 year spin up experiment that was forced by the same forcings as in the CONTROL experiment.

Table S1: Summary of numerical experiments

Experiments	Boundary conditions	
CONTROL	Monthly climatological sea surface temperature (SST) and sea ice extent (SIE) averaged over the period 1964 to 1993, using HadISST[25] with anthropogenic greenhouse gases (GHG) concentrations set at mean values over the same period, and anthropogenic aerosol (AA) precursor emissions[30] at mean values over the period 1970-1993.	32 years
ALL	Monthly climatological SST/SIE averaged over the period of 1996 to 2011, with GHG concentrations set at mean values over the period 1996-2009, and AA precursor emissions at mean values over the period 1996-2010.	27 years
SSTGHG	Monthly climatological SST/SIE averaged over the period of 1996 to 2011, with GHG concentrations set at mean values over the period 1996-2009, but with AA precursor emissions at mean values over the period 1970-1993.	27 years
SSTONLY	Monthly climatological SST/SIE averaged over the period of 1996 to 2011, with GHG concentrations and AA precursor emissions the same in the CONTROL experiment.	27 years
GHGAA	Monthly climatological SST/SIE averaged over the period 1964 to 1993, but with GHG concentrations set at mean values over the period 1996-2009, and AA precursor emissions at mean values over the period 1996-2010.	27 years
GHGONLY	As in the GHGAA experiment, but with AA precursor emissions at mean values over the period 1970-1993.	27 years

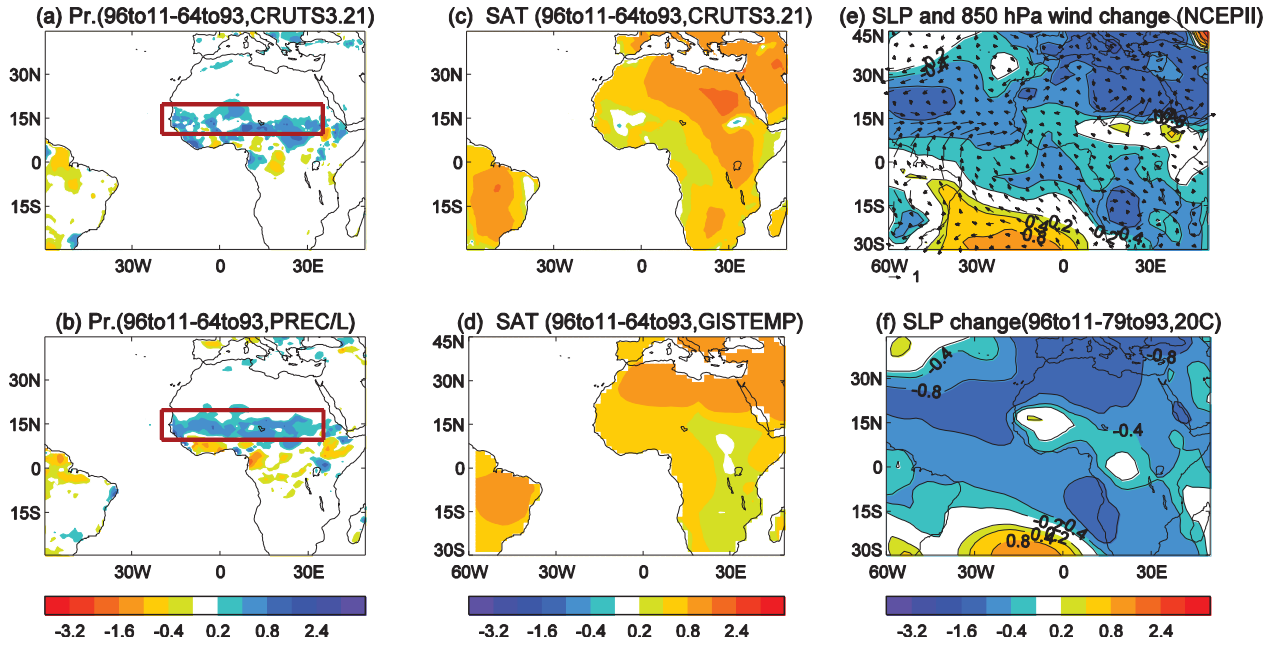

Figure S1. Spatial patterns of seasonal mean (JAS) changes in observations/reanalysis. a-b, Precipitation changes (mm day^{-1}) between the periods 1964-93 and 1996-2011, based on CRUTS3.21 and NOAA PREC/L data sets. **c-d,** SAT differences (^{o}C) between the same periods, based on CRUTS3.21 and GISTEMP data sets. **e,** SLP (hPa) and 850 hPa wind difference for NCEP reanalysis 2 (1996-2011 minus 1979-1993). **f,** SLP (hPa) difference for the 20th century reanalysis (1996-2011 minus 1979-1993). In panel **e** and **f**, the period 1979-93 is used in preference to 1964-93 as the base period as 1979 is the year when significant amounts of satellite data first became available – see Methods.

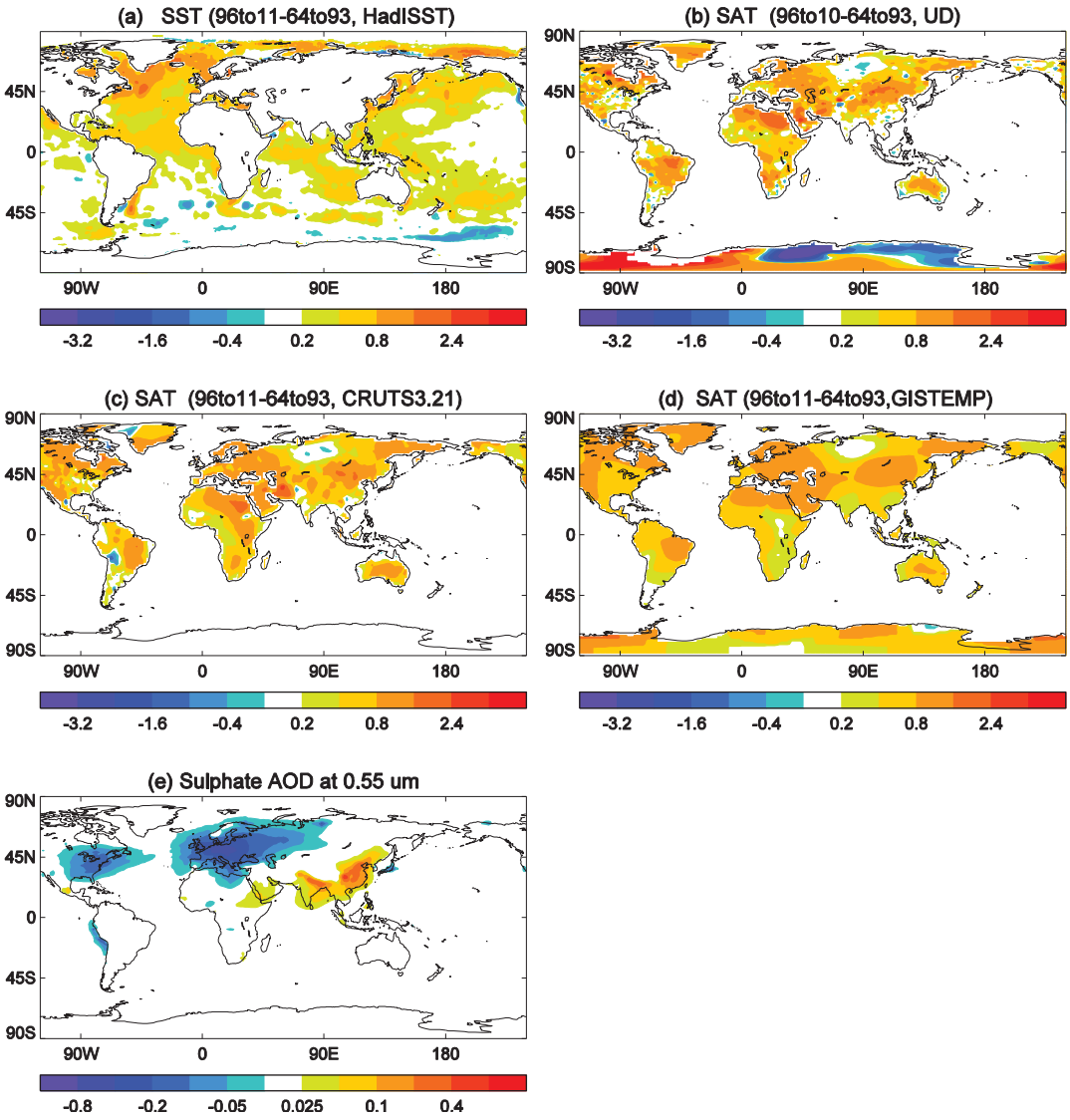

Figure S2. The spatial patterns of global mean changes in JAS between the two periods of 1996-2011 (1996-2010 for UD data) and 1964-1993. a, SST anomalies (°C) based on HadISST. **b-d,** SAT anomalies (°C) based on University of Delaware, CRUTS3.21, and GISTEMP data sets. **e,** The change in sulphate aerosol optical depth (AOD) at 0.55 um between two experiments (ALL–CONTROL).

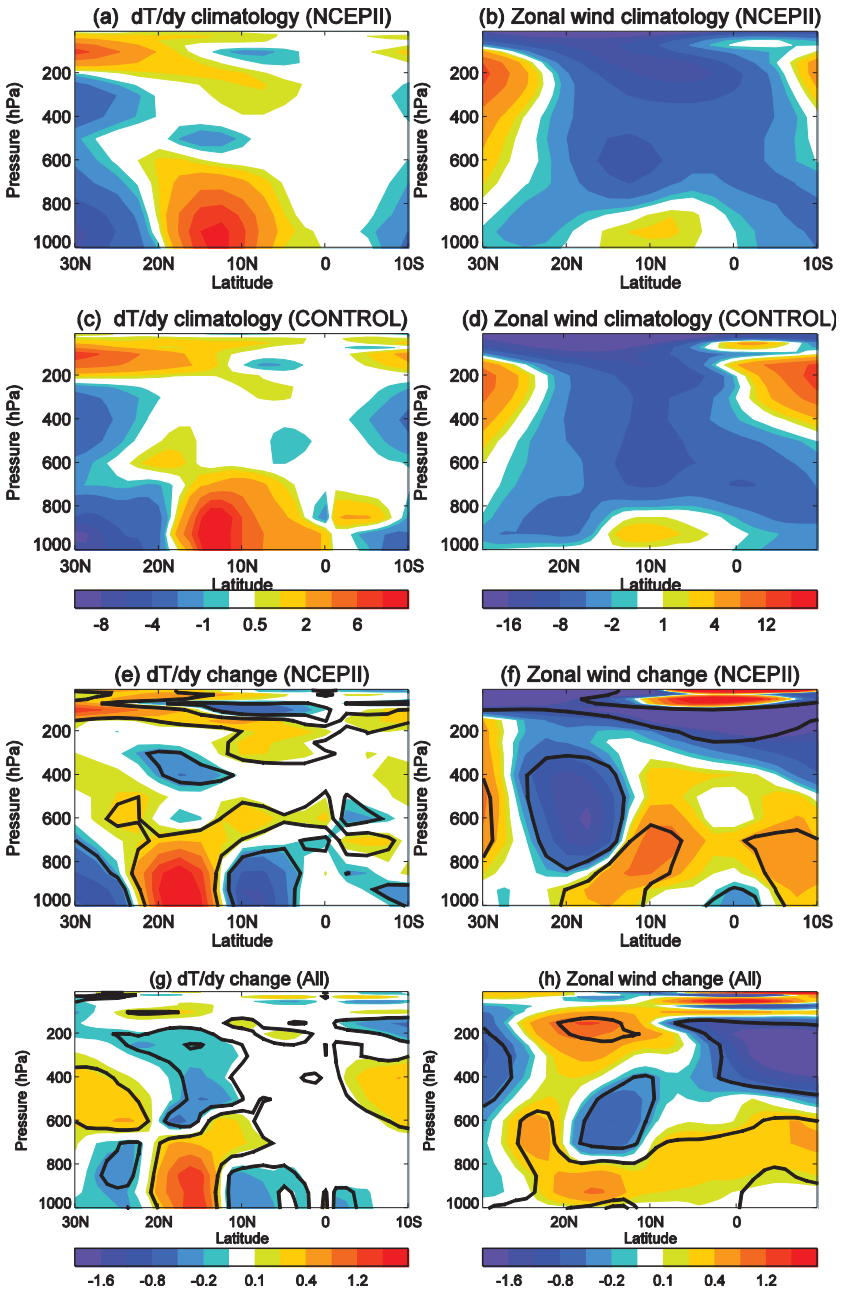

Figure S3: Observed and model simulated seasonal mean (JAS) and zonally (20ºW-35ºE) averaged variables. a-b, Climatological meridional temperature gradient dT/dy (ºC per 1000 km) and zonal wind (m s^{-1}) for the NCEP reanalysis 2 (1979-2011). **c-d,** The same as in **a-c**, but for the model CONTROL simulation. **e-f,** The same as in **a-b**, but for the changes between the two periods of 1996-2011 and 1979-1993 for the NCEP reanalysis 2. **g-h,** The same as in **e-f**, but for the model responses to the changes in SST/SIE, GHG concentrations, and AA precursor emissions (ALL–CONTROL). Thick lines highlight regions where the differences are statistically significant at the 90% confidence level using a two-tailed Student t-test.

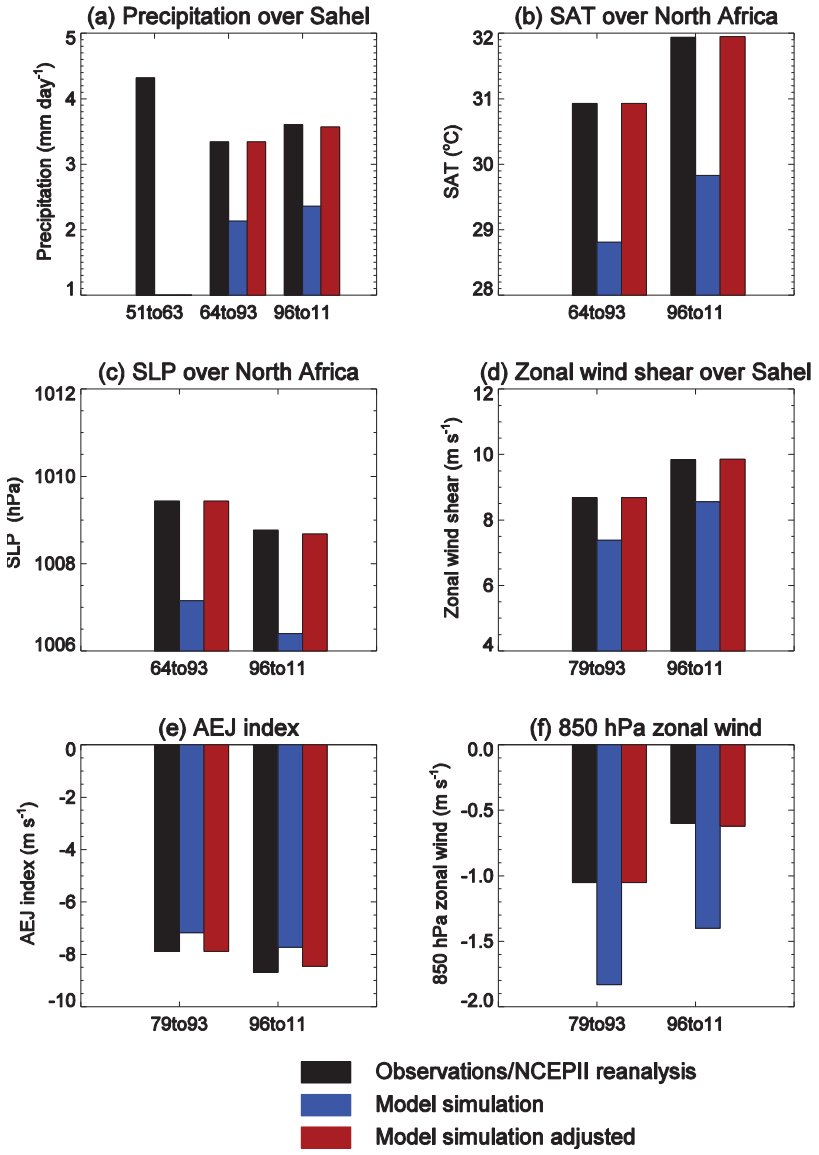

Figure S4: Observed and model simulated seasonal mean (JAS) and area averaged monsoon indices for the Sahel drought period and the recent wetter period. Model results are from the CONTROL and ALL experiments respectively. **a-b,** Precipitation (mm day^{-1}) over the Sahel (the observed value for the period 1951-1963 is also shown) and SAT (^{o}C) over North Africa based on University of Delaware data sets. **c,** SLP (hPa) over North Africa based on the 20th century reanalysis, **d-f**, Vertical zonal wind shear (m s^{-1}) between 925hPa and 600 hPa over the Sahel, African Easterly Jet (AEJ, m s^{-1}), defined as area averaged zonal wind at 600 hPa over the Sahel, and zonal wind (m s^{-1}) at 850 hPa over the Sahel based on NCEP reanalysis 2. Note the late period is 1996-2010 for precipitation and SAT and the early dry period for zonal wind shear and zonal wind is 1979-1993 for the reanalysis. The model adjusted values are the values with the model bias in the 1964-1993 simulation corrected.

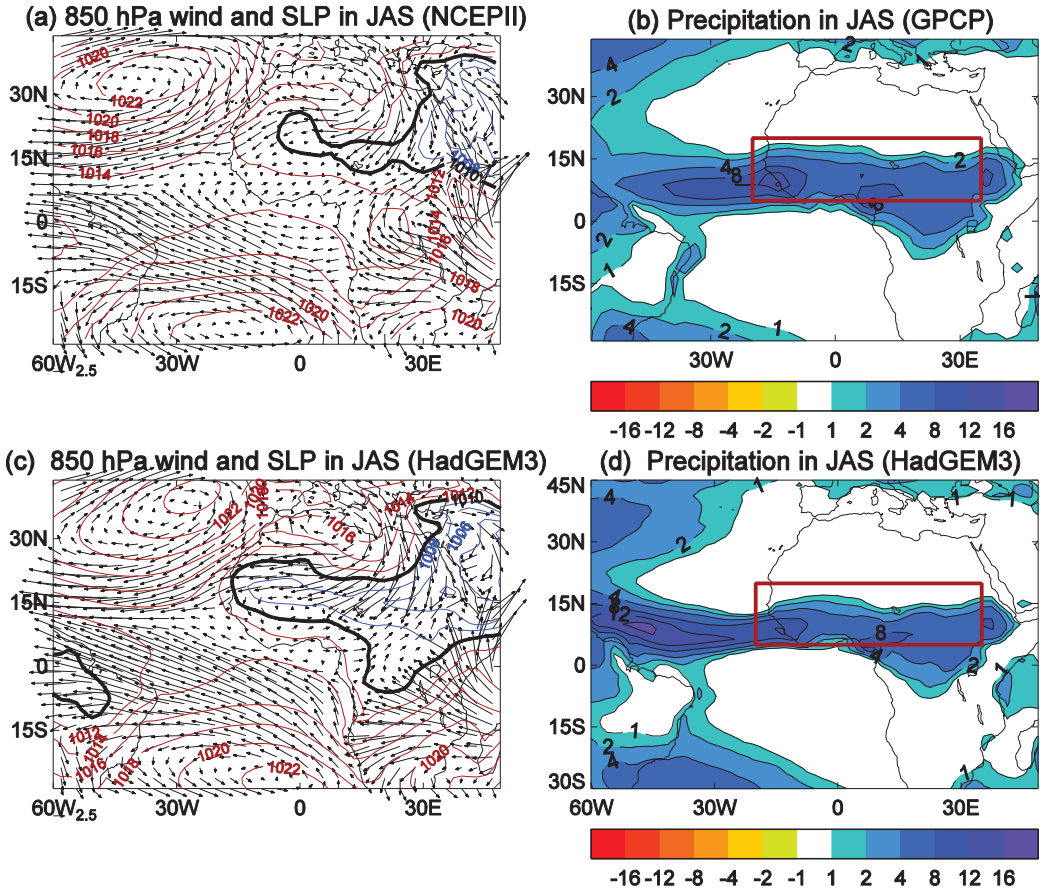

Figure S5. The spatial patterns of JAS climatology for observations and model simulation. **a-b,** SLP (hPa) and 850 hPa winds (m s^{-1}) for NCEP reanalysis 2, and precipitation (mm day^{-1}) for GPCP v2.2 (1979-2011). **c-d,** The same as in **a-b** but for the model CONTROL experiment.

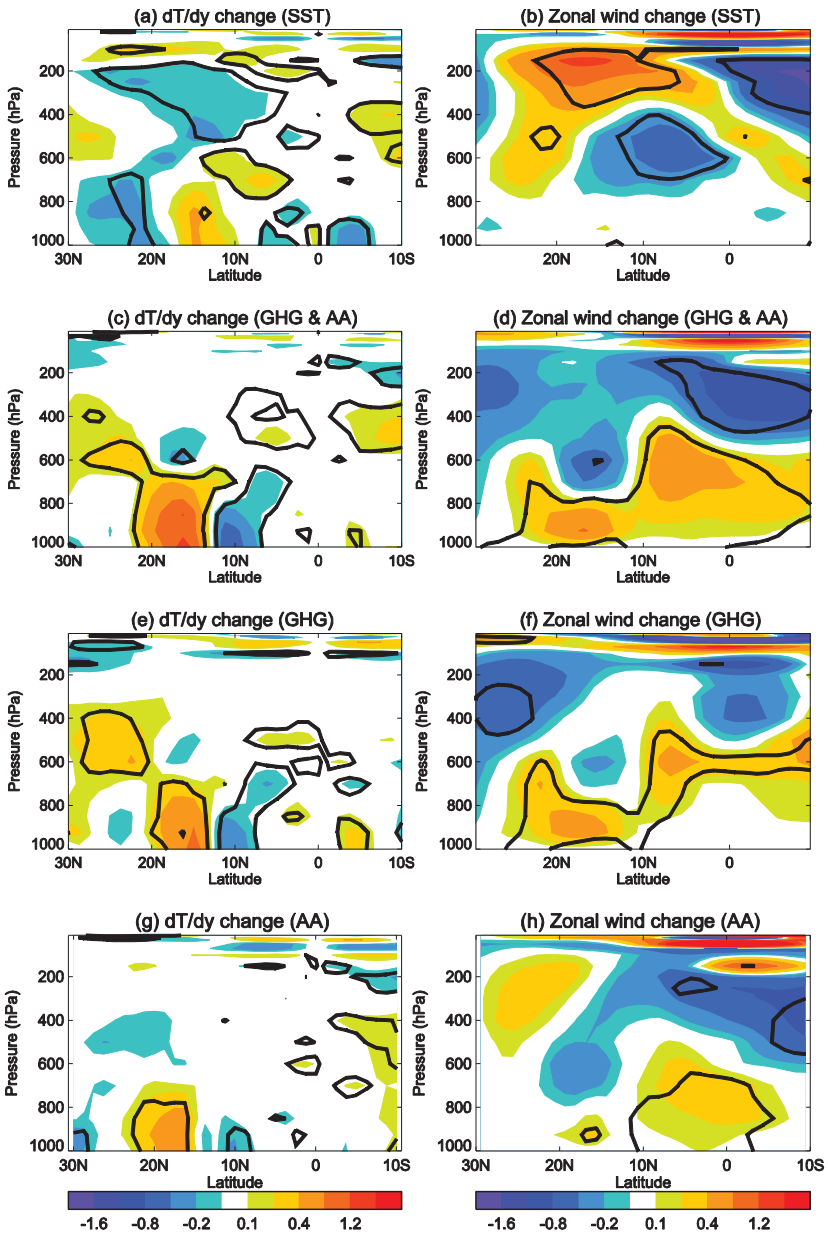

Figure S6: Model simulated seasonal mean (JAS) and zonally (20°W-35°E) averaged changes in response to different forcings. a-b, Changes in meridional temperature gradient dT/dy (°C per 1000 km) and zonal wind (m s^{-1}) for the responses to the changes in SST/SIE (SSTONLY–CONTROL). **c-d,** The same as in **a-b**, but for the responses to changes in GHG concentrations and AA precursor emissions (ALL–SSTONLY). **e-f,** The same as in **a-b**, but for the responses to changes in GHG concentrations (SSTGHG–SSTONLY). **g-h,** The same as in **a-b**, but for the responses to changes in AA precursor emissions (ALL–SSTGHG). Thick lines highlight regions where the differences are statistically significant at the 90% confidence level using a two-tailed Student t-test.

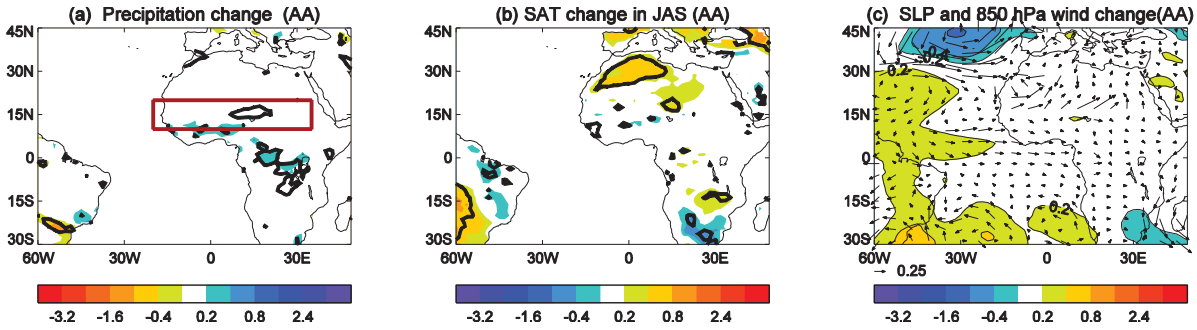

Figure S7: Model simulated seasonal mean (JAS) responses to changes in AA precursor emissions (ALL–SSTGHG). a-c, Seasonal mean (JAS) changes in precipitation (mm day^{-1}), SAT (^{o}C), SLP (hPa) and 850 hPa wind (m s^{-1}). Thick lines in **a and b** highlight regions where the differences are statistically significant at the 90% confidence level using a two-tailed Student t-test.

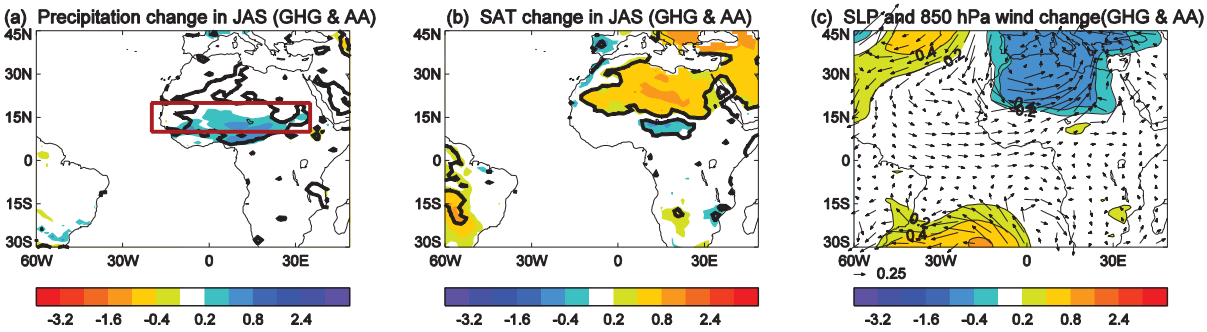

Figure S8: Model simulated seasonal mean (JAS) responses to changes in GHG and AA precursor emissions (GHGAA–CONTROL) in the context of the drought period SSTs. a-c, Seasonal mean (JAS) changes in precipitation (mm day^{-1}), SAT (^{o}C), SLP (hPa) and 850 hPa wind (m s^{-1}). Thick lines in **a and b** highlight regions where the differences are statistically significant at the 90% confidence level using a two-tailed Student t-test.

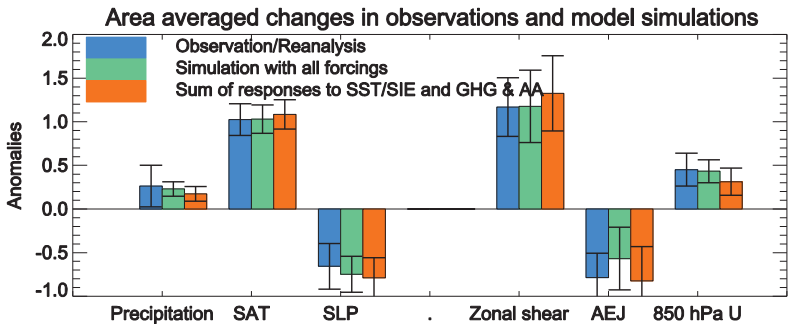

Figure S9: Observed and model simulated seasonal mean (JAS) changes in Sahel rainfall and related variables. Observed changes and simulated responses to changes in all forcings are the same as in Figure 2a and compared with the sum of the response to changes in SST/SIE (SSTONLY–CONTROL) and the response to changes in GHG concentrations and AA precursor emissions in the context of the drought period SST (GHGAA–CONTROL). The coloured bars indicated the central estimates and the whiskers show the 5-95% confidence intervals of the seasonal mean changes in both observations and model experiments based on a two tailed Student t-test. See Methods for details of data sets and model experiments, and analysis and figure 2 caption for various indices.

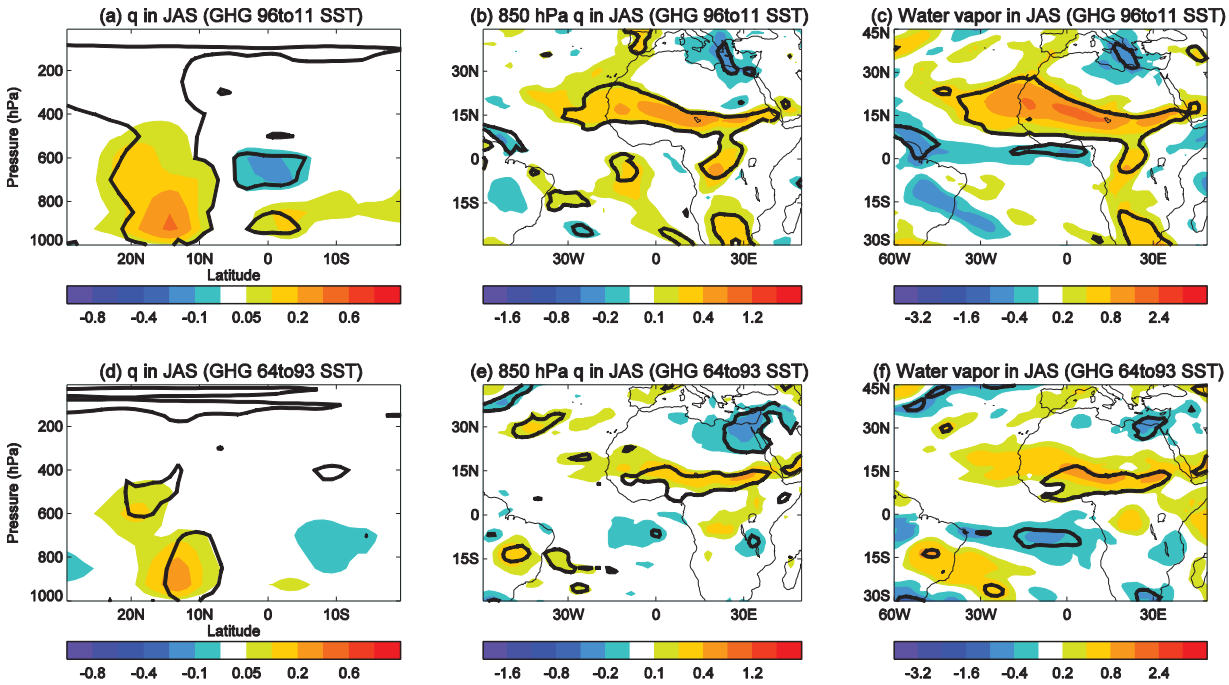

Figure S10: Model simulated seasonal mean (JAS) responses to changes in GHG. a-c, Responses in the context of the recent period SSTs (SSTGHG-SSTONLY). **d-f,** Responses in the context of the drought period SSTs (GHGONLY-CONTROL). **a and d**, Seasonal mean (JAS) changes in zonally averaged (20ºW -35ºE) specific humidity (g kg^{-1}). **b, and e,** Seasonal mean changes in specific humidity (g kg^{-1}) at 850 hPa**. c and f,** Seasonal mean changes in column integrated water vapor (kg m^{-2}). Thick lines highlight regions where the differences are statistically significant at the 90% confidence level using a two-tailed Student t-test.